

IMPROVEMENT OF $\text{La}_{0.65}\text{Sr}_{0.3}\text{MnO}_{3-\delta}$ -YSZ CATHODES BY INFILTRATING NANO $\text{Sm}_{0.6}\text{Sr}_{0.4}\text{CoO}_{3-\delta}$ PARTICLES

Chun Lu, Tal Sholklapper, Xuan Chen, Xiaofeng Zhang,
Craig P. Jacobson, Steven J. Visco, and Lutgard C. DeJonghe
Lawrence Berkeley National Laboratory
Materials Science Division
1 Cyclotron Road, Building 62R0203
Berkeley, CA 94720

ABSTRACT

$\text{La}_{0.65}\text{Sr}_{0.3}\text{MnO}_{3-\delta}$ -YSZ cathodes are infiltrated with $\text{Sm}_{0.6}\text{Sr}_{0.4}\text{CoO}_{3-\delta}$ (SSC) at 800°C using a precipitation method. The effect of SSC infiltration has been characterized for symmetric cells and single cells at reduced temperatures. With SSC addition the cathode polarization resistance, determined from symmetric-cell measurements, significantly decreases: from ~ 19.8 to $8.5\Omega\cdot\text{cm}^2$ at 600°C, and from 7.7 to $3.3\Omega\cdot\text{cm}^2$ at 650°C. Consequently, the single-cell performance with 97% H_2 +3% H_2O fuel is dramatically improved, which may be attributed to the superior electrocatalytic activity of SSC in the cathodes.

INTRODUCTION

Most state-of-art solid oxide fuel cells (SOFC) use 8mol% yttria stabilized zirconia (YSZ) as the electrolyte, Ni-YSZ as the anode, and $\text{La}_{1-x}\text{Sr}_x\text{MnO}_{3-\delta}$ (LSM)-YSZ as the cathode (1). Due to the limited performance of the electrolyte and electrodes at low temperatures (<700°C), cells have been operated at high temperatures (800°C-1000°C). Lowering cell-operation temperatures will expand the materials selection, suppress the degradation of SOFC components, and consequently extend cell lifetime. Therefore, thin-film electrolytes as well as alternative electrolytes with higher oxide-ion conductivity than that of YSZ have been extensively explored to reduce cell ohmic loss at reduced temperatures (2-6). However, at low temperatures cathode polarization leads may lead to a significant cell-performance loss because the electrochemical reaction rates decrease dramatically (7). To improve cathode performance at reduced temperatures, alternative cathode materials including $\text{Sm}_{0.6}\text{Sr}_{0.4}\text{CoO}_{3-\delta}$ (SSC) have been developed (8). Unfortunately, due to the thermal expansion mismatch with YSZ and deleterious reactions with YSZ during high-temperature processing steps, it is difficult to apply SSC directly to YSZ-based cells to form the cathode.

To take advantage of SSC in reduced-temperature cathodes in YSZ-based cells, this work investigated SSC infiltration into porous LSM-YSZ cathodes at 800°C using a precipitation-infiltration method. The effect of SSC addition on the cathode polarization and cell performance at reduced temperatures (600°C-650°C) is reported.

EXPERIMENTAL

YSZ powder (Tosoh-Zirconia; TZ-8Y) was ball milled in isopropanol alcohol (IPA) for 24 hours, using fish oil as the dispersant. Polyvinylbutyral and dibutylphthalate (DBT) binders were then added to the solution that was additionally milled for 1 hr. The solution was dried under a heat lamp, and the dried powder was ground and sieved down to 150 microns. 3g of the sieved powder were pressed in a metal die with a diameter of 1.5 inch. The resultant discs were sintered at 1400°C for 4 hrs to obtain dense YSZ discs with a diameter of ~1.19 inch. Symmetric cells were prepared using an aerosol spray method (6). YSZ and $\text{La}_{0.65}\text{Sr}_{0.3}\text{MnO}_{3-\delta}$ (Praxair Specialty Ceramics) (50:50 wt%) were attrition milled in IPA with the addition of fish oil and DBT to form a suspension. The suspension was then sonicated for 5 mins, and sprayed on both sides of YSZ discs to form symmetric cells having 1cm^2 electrodes. The electrodes were then sintered at 1150°C for 4 hrs to obtain porous LSM-YSZ electrodes.

Single cells in this work were fabricated by tape casting (5). Nickel oxide (NiO; J. T. Baker) and YSZ (50:50 wt%) powders were thoroughly mixed in water using Duramax D3005 as the dispersant. Duramax B1000 and HA-12 binders were then added to form NiO-YSZ slurry. After evaporation of excessive water, the slurry was cast onto a mylar film and dried at ambient temperature. The green tape was then cut into circular discs with a diameter of 1.5 inch, and preheated at 1100°C for 2 hrs. The YSZ electrolyte and LSM-YSZ cathode with an active area of 1cm^2 were placed onto the NiO-YSZ anode support using the aerosol spray method described above. Based on SEM characterization of single cells (not shown), the cell component thickness is $\sim 300\mu\text{m}$, $\sim 10\mu\text{m}$, and $\sim 30\mu\text{m}$ for the anode, the electrolyte, and the cathode, respectively.

A precipitation-infiltration method was used to insert SSC or additional LSM into the porous LSM-YSZ electrodes. Aqueous solution containing urea and Sm, Sr, Co nitrates in the ratio of 0.6:0.4:1 or La, Sr, Mn nitrates in the ratio of 0.65:0.3:1 was absorbed to saturation into the porous LSM-YSZ electrodes. The sample was heated at 90°C for 2 hrs and fired at 800°C for 2hrs. The phase formation of SSC and LSM was examined using a diffractometer (Siemens D-500) with CuK_α radiation in the 2θ range from 20° to 80°. The morphologies of SSC in the porous cathode were observed using a PHILIPS CM200 TEM.

Platinum current collectors were placed on the electrodes of both symmetric and single cells, and were fired at 800°C for 2 hrs. In the case of symmetric cells, the electrode polarization resistance was measured under open circuit voltage (OCV) condition in air using a Solartron 1260 frequency response analyzer interfaced with a Solartron 1286 electrochemical interface. The single cells were sealed onto an alumina tube using Aremco-516 cement. Cell I-V curves with 97% H_2 +3% H_2O as the fuel and air as the oxidant were collected using LabView software, and cell impedance spectra were characterized as well.

RESULTS AND DISCUSSION

Fig. 1 shows the XRD patterns of the prepared SSC and LSM powders after sintering at 800°C for 2hrs. The majority of the peaks correspond to the perovskite phase,

although there are some peaks indicating the presence of metal oxides. Hence, this precipitation method makes it possible to incorporate SSC or LSM into LSM-YSZ cathodes at low temperatures and, in the case of SSC, significantly suppress its adverse reactions with YSZ.

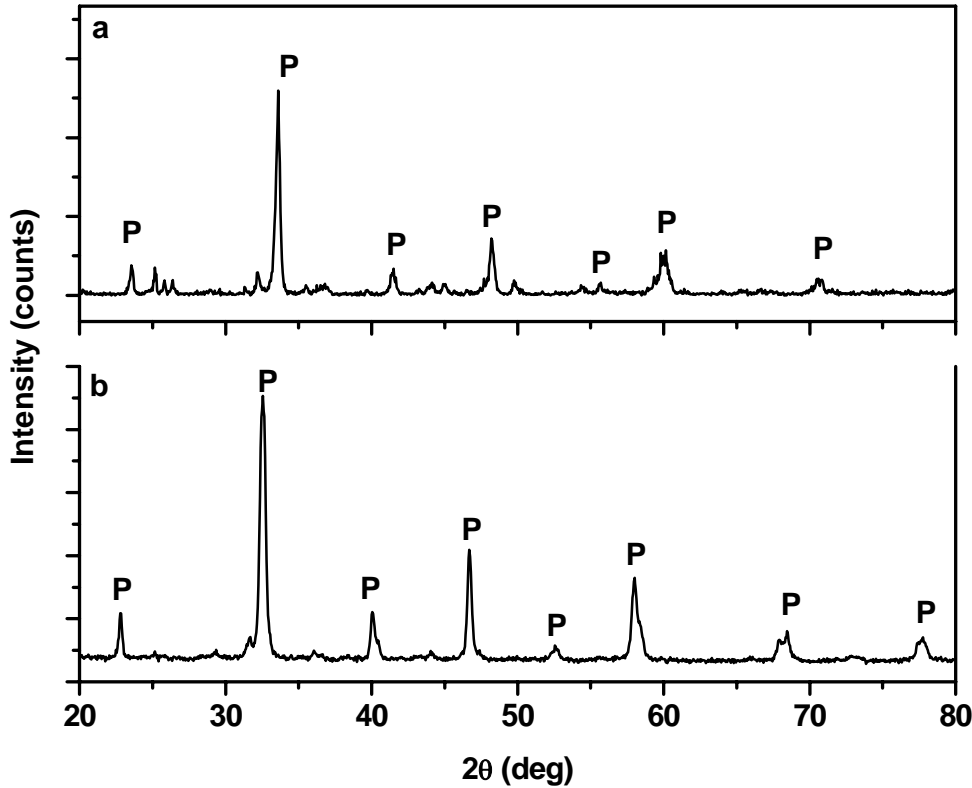


Fig. 1 XRD patterns of the prepared (a) SSC (b) LSM powders sintered at 800°C for 2hrs. (P) Peaks corresponding to perovskite phase

Fig. 2 displays the impedance spectra of LSM-YSZ/YSZ/LSM-YSZ symmetric cells with and without infiltrated species, at 600°C and 650°C. All spectra show a relatively small high-frequency lobe (HFL) and a dominant low-frequency lobe (LFL). The cell ohmic resistance in the spectra is truncated for comparison, and the electrode polarization resistance (R_p) is directly determined from the spectra as illustrated (9). With the infiltrated SSC in the LSM-YSZ electrode, both the HFL and LFL are strongly decreased. Consequently R_p is reduced from ~ 19.8 to $8.5 \Omega \cdot \text{cm}^2$ at 600°C, and 7.7 to $3.3 \Omega \cdot \text{cm}^2$ at 650°C. This indicates that the modified LSM-YSZ cathode with the infiltrated SSC particles could be expected to exhibit better electrochemical performance at reduced temperatures.

Infiltrating SSC into LSM-YSZ cathodes indeed enhances the cell performance significantly, as shown in Fig. 3. The cell OCVs are 1.13V at 600°C and 1.11V at 650°C, suggesting that the cells were well sealed. The cell maximum powder density is considerably increased from 80 mW/cm^2 to 153 mW/cm^2 at 600°C, and 162 mW/cm^2 to

270mW/cm² at 650°C. The SSC addition noticeably changes the curvature of the IV plots under the low current density range. The slopes of the IV curves for the cell with the LSM-YSZ cathode having SSC are less steep. This implies the presence of SSC in the cathode improves the electrochemical reactions along the cathode-electrolyte interface. This interpretation is supported by the impedance measurement results shown in Fig. 4. The single-cell impedance curves have shapes similar to those of the symmetric cells (Fig. 2). This evidences that the cathode likely controls the overall cell performance at low temperatures, which is consistent with the conclusions in the literatures (3, 8, 9). At 600°C the cell total resistance (R_t) (the intercept of the impedance spectrum on the real axis at low frequency) declines from ~9.9 to 3.3Ω·cm² when SSC is included into the LSM-YSZ cathode. Similarly R_t drops from 4.6 to 1.9Ω·cm² at 650°C. The smaller R_t accounts for the better performance when SSC exists in the LSM-YSZ cathode.

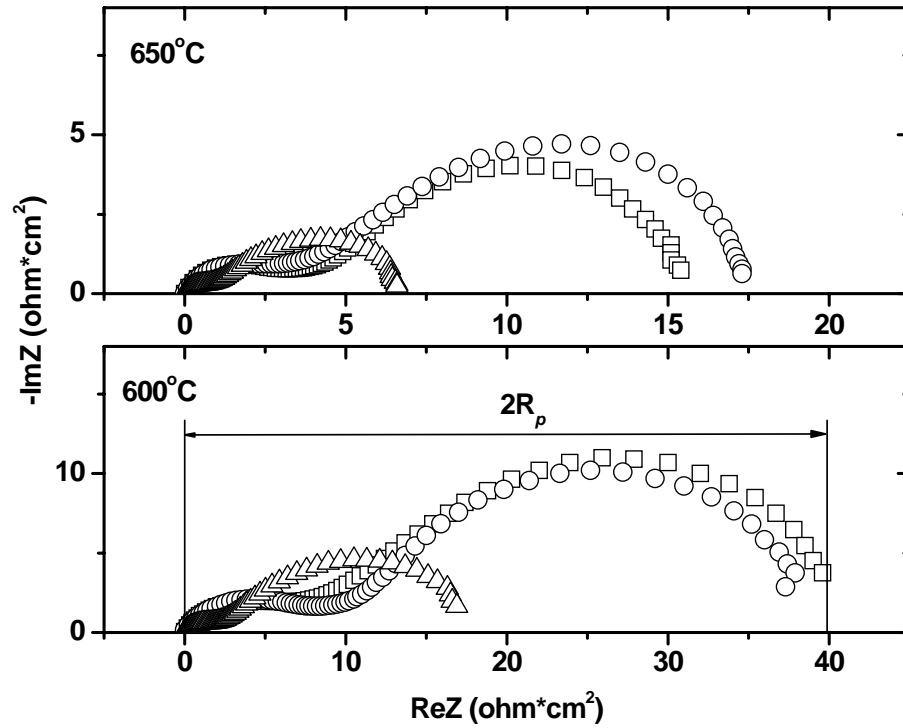


Fig. 2 Impedance spectra of symmetric LSM-YSZ/YSZ/LSM-YSZ cells (square) with infiltrated LSM (circle) and SSC (triangle).

The effective charge transfer resistance (R_{ct}^{eff}) of a composite electrode can be expressed as (10)

$$R_{ct}^{eff} = \sqrt{\frac{R_{ct}L}{\sigma_{O^{2-}}(1-P)}}$$

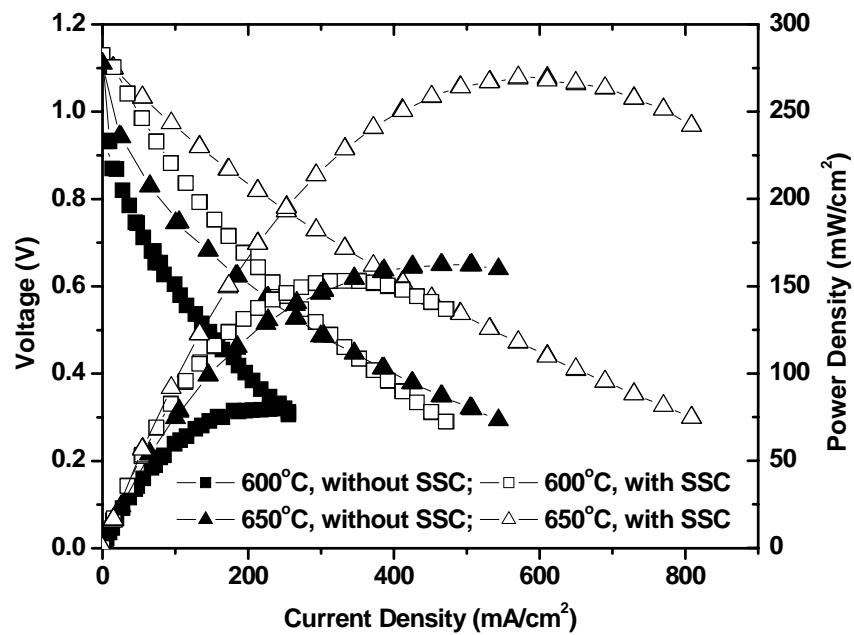


Fig. 3 Effect of infiltrated SSC into LSM-YSZ cathodes on cell performance curves at 600°C and 650°C.

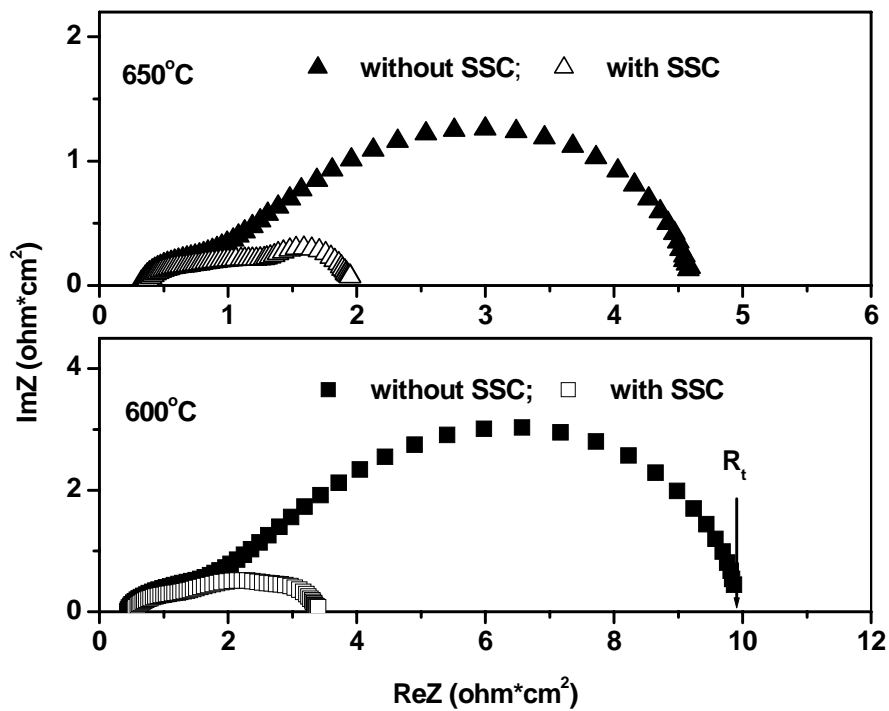


Fig. 4 Effect of infiltrated SSC into LSM-YSZ cathodes on cell impedance spectra at 600°C and 650°C.

in which R_{ct} is the intrinsic charge transfer resistance; L is the grain size of the material and P is the electrode porosity; and $\sigma_{O^{2-}}$ is the ionic conductivity of electrolyte phase. Based on this model, the cathode performance has been increased by optimizing microstructures (10), improving the ion-conductivity (11) and introducing electrocatalysts such as Pt (7). Since in this study only small amounts of SSC (~ 0.5 mg) were added to the LSM-YSZ cathode at 800°C , one could reasonably assume that the SSC does not dramatically affect L , P and $\sigma_{O^{2-}}$. This is partially reinforced by the fact that infiltrating LSM particles into the LSM-YSZ cathode barely changes the electrode polarization resistance as shown in Fig. 2.

Fig. 5 is a TEM image showing an infiltrated SSC particle in a porous LSM-YSZ structure with a size of ~ 40 to 60 nm. The particles most likely reduce R_{ct} that depends on the kinetics of oxygen diffusion and surface exchange in a composite cathode (12,13), because SSC has superior kinetic properties compared with LSM (3,14). For instance, the surface exchange coefficient of SSC is approximately two orders higher than that of LSM at low temperatures (3). The SSC is expected to play a similar role as Pt particles exert in LSM-YSZ cathodes. That is, SSC facilitates the dissociation of O_2 molecules to form adsorbed oxygen atoms around the triple phase boundaries, and/or the sequential exchange reaction between oxygen atoms and oxygen vacancies in the LSM (7). Therefore, the presence of SSC in the LSM-YSZ cathode reduces R_{ct} , and R_{ct}^{eff} accordingly. The decreased R_{ct}^{eff} leads to the smaller polarization resistances (Fig. 2) so that the modified LSM-YSZ cathode here remarkably improves the cell performance at 600°C and 650°C .

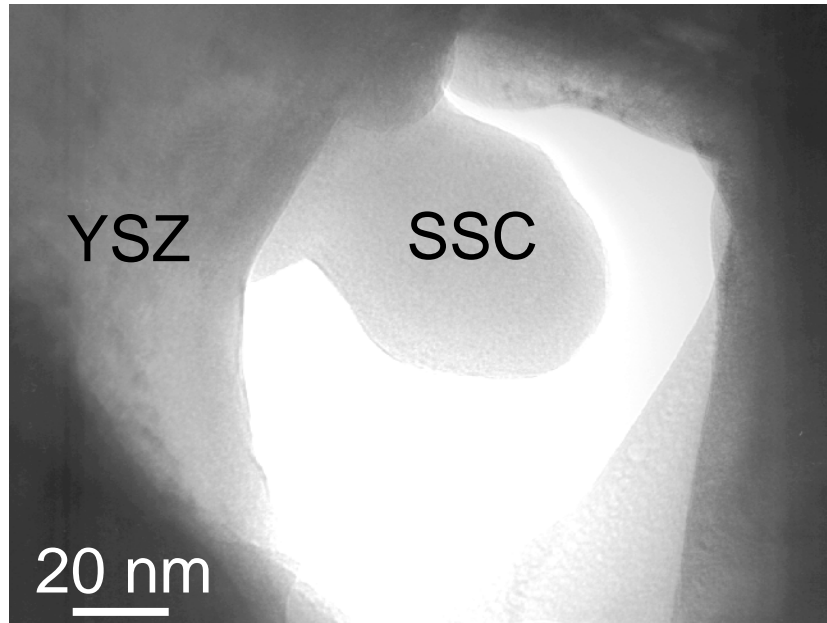


Fig. 5 A TEM image of an infiltrated SSC particle in a LSM-YSZ cathode.

CONCLUSIONS

It has been demonstrated that conventional LSM-YSZ cathodes at reduced temperatures can be made to operate more effectively by infiltrating SSC catalyst particles, using a process that does not exceed 800°C. Electrochemical characterization at 600°C and 650°C of symmetric and single cells indicates that the SSC infiltration largely decreases the cathode polarization resistance and improves the cell performance correspondingly.

ACKNOWLEDGEMENTS

This work was supported by the U. S. Department of Energy, through the National Energy Technology Laboratory.

REFERENCES

1. N. Q. Minh and T. Takahashi, *Science and Technology of Ceramic Fuel Cells*, Elsevier 1995.
2. K. Huang, R. Tichy, J. B. Goodenough and C. Milliken, *J. Am. Ceram. Soc.*, **81** (10) 2581 (1998).
3. R. Doshi, V. Richards, J. D. Carter, X. Wang, and M. Krumpelt, *J. Electrochem. Soc.*, **146** (4), 1273 (1999).
4. C. Xia, F. Chen and M. Liu, *Electrochemical and Solid-State Letters*, **4** (5) A52 (2001).
5. C. Wang, W. L. Worrell, S. Park, J. M. Vohs, R. J. Gorte, *J. Electrochem. Soc.*, **148** (8), A864 (2001).
6. S. De Souza, S. J. Visco, and L. C. DeJonghe, *J. Electrochem. Soc.*, **144**, L35 (2002).
7. H. Uchida, S. Arisaka, and M. Watanabe, *J. Electrochem. Soc.*, **149** (1), A13 (2002).
8. J. M. Ralph, C. Rossignol, and R. Kumar, *J. Electrochem. Soc.*, **150** (11), A1518 (2003).
9. C. Xia, Y. Zhang, and M. Liu, *Electrochemical and Solid-State Letters*, **6** (12) A290 (2003).
10. C. Tanner, K. Fung, and A. Virkar, *J. Electrochem. Soc.*, **144**, 21 (1997).
11. S. Jiang, Y. Leng, S. Chan, and K. Khor, *Electrochemical and Solid-State Letters*, **6** (4) A67 (2003).
12. B. C. H. Steel, K. M. Hori, and S. Uchino, *Solid State Ionics*, **135**, 445 (2000).
13. S. B. Adler, J. A. Lane, B. C. H. Steele, *J. Electrochem. Soc.*, **143**, 3554 (1996).
14. R. A. De Souza, and J. A. Kilner, *Solid State Ionics*, **126**, 153 (1999).